OPEN ACCESS Freely available online

PLoS one

A Protein Aggregation Based Test for Screening of the Agents Affecting Thermostability of Proteins

Tatyana Eronina[1]*, Vera Borzova[1], Olga Maloletkina[1], Sergey Kleymenov[2], Regina Asryants[3], Kira Markossian[1], Boris Kurganov[1]*

1 Bach Institute of Biochemistry, Russian Academy of Sciences, Moscow, Russia, **2** Kol'tsov Institute of Developmental Biology, Russian Academy of Sciences, Moscow, Russia, **3** Belozersky Institute of Physico-Chemical Biology, Moscow State University, Moscow, Russia

Abstract

To search for agents affecting thermal stability of proteins, a test based on the registration of protein aggregation in the regime of heating with a constant rate was used. The initial parts of the dependences of the light scattering intensity (I) on temperature (T) were analyzed using the following empiric equation: $I = K_{agg}(T-T_0)^2$, where K_{agg} is the parameter characterizing the initial rate of aggregation and T_0 is a temperature at which the initial increase in the light scattering intensity is registered. The aggregation data are interpreted in the frame of the model assuming the formation of the start aggregates at the initial stages of the aggregation process. Parameter T_0 corresponds to the moment of the origination of the start aggregates. The applicability of the proposed approach was demonstrated on the examples of thermal aggregation of glycogen phosphorylase *b* from rabbit skeletal muscles and bovine liver glutamate dehydrogenase studied in the presence of agents of different chemical nature. The elaborated approach to the study of protein aggregation may be used for rapid identification of small molecules that interact with protein targets.

Citation: Eronina T, Borzova V, Maloletkina O, Kleymenov S, Asryants R, et al. (2011) A Protein Aggregation Based Test for Screening of the Agents Affecting Thermostability of Proteins. PLoS ONE 6(7): e22154. doi:10.1371/journal.pone.0022154

Editor: Darren R. Flower, Aston University, United Kingdom

Received December 16, 2010; **Accepted** June 19, 2011; **Published** July 8, 2011

Funding: This study was funded by the Russian Foundation for Basic Research (grants 11-04-00932-?, 11-04-01271-a and 11-04-01350-?), the Program "Molecular and Cell Biology" of the Presidium of the Russian Academy of Sciences and Dmitry Zimin Dynasty Foundation, the Federal Target Program "Scientific and Scientific-Pedagogical Personnel of Innovative Russia" in 2009–2013 (the state contract No. P1356). The funders had no role in study design,data collection and analysis, decision to publish, or preparation of the manuscript.

Competing Interests: The authors have declared that no competing interests exist.

* E-mail: eronina@inbi.ras.ru (TE); kurganov@inbi.ras.ru (BK)

Introduction

Senisterra and coworkers [1,2] elaborated a high-throughput light-scattering-based method for screening of ligands specifically interacting with protein targets. Thermal protein denaturation is used to characterize the binding of ligands to their target protein. This method is based on the assumption that the proteins under study irreversibly denaturate and form aggregates during thermal denaturation. Light scattering as a measure of protein aggregation is a very sensitive technique. Protein aggregation is studied in the regime of heating with a constant rate. The dependence of the light scattering intensity on temperature has a sigmoid shape. At rather high temperatures the light scattering intensity (I) reaches a limiting value (I_{lim}). To characterize thermostability of a protein, Senisterra and coworkers used the temperature (T_{agg}) corresponding to the middle point of the transition, i.e., a temperature at which $I = I_{lim}/2$. Parameters I_{lim} and T_{agg} are determined by fitting of the experimental dependence of I on temperature with the following empiric equation, analogous to the Boltzmann equation:

$$I = \frac{I_{lim}}{1+\exp[(T_{agg}-T)/B]}, \qquad (1)$$

where B is a constant.

According to the idea advanced by Senisterra and coworkers a change in the T_{agg} value in the presence of a ligand characterizes the effect of the latter on protein thermostability. To substantiate this conclusion, the authors additionally used differential scanning calorimetry (DSC), which is a source of direct information on the protein resistance to high-temperature exposure. The authors also constructed a plot demonstrating the existence of a correlation between the T_{agg} value and the position of the maximum on the DSC profiles (T_m).

It is evident that the accuracy of determining parameter T_{agg} is connected with the reliability of the estimation of parameter I_{lim}. When trying to estimate parameter I_{lim} we should take into account that the "true" limiting level of the light scattering intensity may not be reached because of precipitation of the large-sized aggregates formed at high temperatures. Such a precipitation results in the decrease in the light scattering intensity, and the real experimental dependence of I on temperature looks like a curve passing through a maximum. The maximum value of the light scattering intensity may be lower than the I_{lim} value calculated from Eq. (1). Besides, the correlation between the increment of the light scattering intensity and the degree of protein denaturation should be controlled not only by checking the correlation between parameters T_{agg} and T_m, but by stricter analysis of the relationship between turbidimetric data and calorimetric data, supplying direct information on the degree of protein denaturation.

To avoid the uncertainty in the estimation of parameter I_{lim}, in the present work we proposed new parameters, which characterize the rate of aggregation. To determine these parameters, there is no

need for the full dependences of the light scattering intensity on temperature, since the proposed parameters (the initial temperature of aggregation and the parameter characterizing the rate of change in the light scattering intensity with temperature) are calculated from the initial parts of the dependences of I on temperature. The use of these parameters allows us to obtain the quantitative characteristics of the effect of the agents to be tested on the rate of aggregation. Since the initial stage of thermal aggregation of the proteins is the stage of denaturation, the ligands under study involve agents affecting both the stage of denaturation and the stage of aggregation. To demonstrate the applicability of the proposed approach, thermal aggregation of glycogen phosphorylase *b* (Ph*b*; EC 2.4.1.1) from rabbit skeletal muscles and bovine liver glutamate dehydrogenase (GDH; EC 1.4.1.3) were used as examples.

Mathematical description of the initial parts of the dependences of the light scattering intensity on temperature

As a preliminary step we discuss the kinetics of thermal aggregation of the proteins registered at a fixed temperature. To analyze the initial parts of the dependences of the light scattering intensity (I) on time, the following empiric equation was proposed [3]:

$$I = K_{agg}(t - t_0)^2. \quad (t > t_0) \tag{2}$$

In this equation K_{agg} is a constant with the dimension of (counts/s)·min^{-2} and t_0 is the duration of the lag period (t_0 is a point in time at which the light scattering intensity begins to increase). The applicability of Eq. (2) was demonstrated for thermal aggregation of Ph*b* [3–5], glyceraldehyde-3-phosphate dehydrogenase (GAPDH; EC 1.2.1.12) [6] and creatine kinase (CK; EC 2.7.3.2) from rabbit skeletal muscles [7]. Parameter K_{agg} characterizes the initial rate of aggregation, and the construction of a dependence of parameter K_{agg} on the initial protein concentration $[P]_0$ allows calculating the order of aggregation with respect to the protein (n) ($K_{agg} = \text{const}\cdot[P]_0^n$). The dependence of parameter K_{agg} on the Ph*b* concentration constructed on the basis of kinetic data for Ph*b* aggregation at 53°C (pH 6.8) was linear [3], and consequently $n = 1$. This is true when the stage of unfolding of a protein molecule proceeds with a substantially lower rate than the following stages of aggregation of the unfolded protein molecules [8,9]. In other words, the rate-limiting stage of the overall process of aggregation is the monomolecular stage of protein unfolding. According to the data presented by Kurganov et al. [10] the kinetic scheme of thermal denaturation of Ph*b* involves a stage of the conformational change of the enzyme dimeric molecule followed by dissociation of the dimer into monomers and denaturation of labile monomeric forms.

The kinetics of thermal aggregation of GDH at various concentrations of the protein was studied by Sabbaghian et al. [11] (50°C; pH 8.0). The order of aggregation with respect to the protein calculated on the basis of these kinetic data is close to unity: $n = 0.8 \pm 0.1$.

The analysis of the data on thermal aggregation of β_L-crystallin from bovine lens at 60°C (pH 6.8) obtained in [12] shows that parameter n is close to 2 ($n = 1.99 \pm 0.07$). It is generally accepted that the initial stage of aggregation is the stage of nucleation [3,8,9,13–19]. The fact that the value of parameter n for thermal aggregation of β_L-crystallin exceeds unity is indicative of the involvement of several molecules of denatured β_L-crystallin in the nucleation process.

Consider a situation when Eq. (2) may be strictly fulfilled. The theoretical analysis carried by Ferrone [16] shows that for the nucleation-dependent aggregation the accumulation of monomers incorporated in the aggregate (Δ) proceeds according to the time-squared law:

$$\Delta = \frac{1}{2} JJ * c * t^2, \tag{3}$$

where $\tilde{J}$ is the elongation rate of aggregates, $\tilde{J}^*$ is the elongation rate of the nucleus and c^* is the concentration of the nuclei. Such an early kinetics of aggregation was demonstrated experimentally, for example, for aggregation of polyglutamine peptides [20], aggregation of a slow-folding mutant of a β-clam protein, cellular retinoic acid-binding protein (P39A CRABP I) [21], and aggregation of protein L [22].

When studying the kinetics of thermal aggregation of some proteins by dynamic light scattering (DLS) we have shown that the hydrodynamic radius (R_h) of the initially registered aggregates (the start aggregates) amounts to tens of nanometers [23]. This means that a start aggregate contains hundreds of denatured protein molecules. We could not detect intermediate states between the original forms of the proteins and the start aggregates. It should be noted that rather low temperatures were selected for the study of protein aggregation in this investigation (37°C for Ph*b* and 45°C for GAPDH). The nuclei formed at the initial stages of aggregation involve several monomers. Therefore one can assume that there is no accumulation of nuclei in the system, and coalescence of the formed nuclei into larger structures, namely start aggregates, takes place. The initial increase in the light scattering intensity is connected with accumulation of the start aggregates, the size of the latter remaining unchanged (the hydrodynamic radius of the start aggregates was designated by $R_{h,0}$). It is evident that in the time interval where the R_h value is constant ($R_h = R_{h,0}$; see [23]) the light scattering intensity is strictly proportional to the amount of the aggregated protein. Thus, in this case Eq. (2) may be used for the quantitative description of the early kinetics of the aggregation process, and parameter K_{agg} is a true measure of the initial rate of aggregation. When protein aggregation is studied at elevated temperatures, the time interval corresponding to the accumulation of the start aggregates is greatly reduced, and the registered increase in the hydrodynamic radius of the protein aggregates at $t > t_0$ is due to the attachment of individual denatured protein molecules to the start aggregates or the sticking of the start aggregates. This results in the additional increment in the light scattering intensity apart from the main contribution accounted for the formation of the start aggregates. Eq. (2) should be treated as an empiric equation where parameter K_{agg} is a rough characteristic of the initial aggregation rate.

When studying the dependences of the hydrodynamic radius of protein aggregates on temperature obtained in the experiments with heating of protein solutions with a constant rate, we observed that the character of these dependences is identical to that for the dependences of the hydrodynamic radius of protein aggregates on time obtained at a fixed temperature [24–26]. Therefore we propose to use the following equation analogous to Eq. (2) for analysis of the initial parts of the dependences of the light scattering intensity on temperature obtained in the regime of heating with a constant rate:

$$I = K_{agg}(T - T_0)^2. \quad (T > T_0) \tag{4}$$

In this equation T_0 is the initial temperature of aggregation, i.e., the temperature at which the light scattering intensity begins to

increase, and K_{agg} is a constant with the dimension of (counts/s)·°C^{-2} Parameter T_0 indicates the moment of origination of the start aggregates, whereas parameter K_{agg} characterizes the rate of aggregation. It was of interest to check the applicability of Eq. (4) for the analysis of protein aggregation in the regime of heating with a constant rate, and to clarify how parameters T_0 and K_{agg} change with variation in the protein concentration.

Materials and Methods

Hepes, glucose 1–phosphate, AMP, trimethylamine N-oxide (TMAO), creatine kinase (CK) from rabbit skeletal muscles, bovine liver GDH, NAD, NADH, ADP, L-glutamate, L-leucine and α-crystallin were purchased from "Sigma" (USA). The concentrations of CK, GDH and α-crystallin were determined from the absorbance at 280 nm using the extinction coefficients $A^{1\%}_{1cm}$ of 8.8 [27], 9.7 [11] and 8.5 [28], respectively. NaCl was purchased from "Reakhim" (Russia), 2-hydroxypropyl-β-cyclodextrin (degree of substitution 3±1) (HP-β-CD) was obtained from CycloLab LTD (Hungary).

Isolation of Phb

Ph*b* was isolated from rabbit skeletal muscles as described in [29]. Ph*b* concentration was determined spectrophotometrically at 280 nm using the extinction coefficient $A^{1\%}_{1cm}$ of 13.2 [30].

Isolation of GAPDH

GAPDH was isolated from rabbit skeletal muscles as described by Scopes and Stoter [31] with an additional purification step using gel-filtration on Sephadex G-100. GAPDH concentration was determined spectrophotometrically at 280 nm using the extinction coefficient $A^{1\%}_{1cm}$ of 10.6 [32].

Differential Scanning Calorimetry

Thermal denaturation of Ph*b* was investigated by DSC using the adiabatic scanning microcalorimeter DASM–4M (Institute of Biological Instruments, Russian Academy of Sciences, Pushchino, Russia) with 0.47 ml capillary platinum cells. All measurements were carried out at the rate of heating by 1°C/min using the temperature range from 20 to 85°C and constant pressure of 2.2 atm. The dependences of the heat power on temperature were calculated using the program Origin software (MicroCal, Inc., USA).

The capillary construction of calorimetric cells prevents the artifacts caused by protein precipitation, which are often observed in batch calorimetric cells as exothermic peaks. In the capillary cells large-sized aggregated particles of protein are unable to settle and stir the solution, so no extra thermal production can arise [33].

Light Scattering Intensity Measurements

DLS measurements were performed on a commercial instrument Photocor Complex (Photocor Instruments Inc., USA; www.photocor.com). An He-Ne laser (Coherent, USA, Model 31-2082, 632.8 nm, 10 mW) was used as the light source. The temperature of sample cell was controlled by the proportional integral derivative (PID) temperature controller to within ±0.1°C. To carry on the light scattering intensity measurements in the regime of heating with a constant rate, a fast thermostat with the uniform distributed heater has been developed. The special design of this compact unit allows simply replacing the standard sample cell holder of the main thermostat of the Photocor Complex setup by the fast thermostat. Fast platinum thermometers with time constant of 1 s have been used both for temperature control and for real-time monitoring of temperature directly in the sample cell. The fast thermostat is fully controlled with the existing PID controller through the macro procedure of the Photocor program. Temperature scanning rate can be assigned from 10°C/min to any slower value.

A quasi-cross correlation photon counting system with two photomultiplier tubes was used to increase the accuracy of particle sizing in the range from 1.0 nm to 5.0 μm. DLS data have been accumulated and analyzed with a multifunctional real-time correlator. DynaLS software (Alango, Israel) was used for polydispersity analysis of DLS data. The diffusion coefficient D of the particles is directly related to the decay rate τ_c of the time-dependent correlation function for the light-scattering intensity fluctuations: $D = 1/2\tau_c k^2$. In this equation k is the wave number of the scattered light, $k = (4\pi n/\lambda)\sin(\theta/2)$, where n is the refractive index of the solvent, λ is the wavelength of the incident light in vacuum and θ is the scattering angle. The mean hydrodynamic radius of the particles, R_h, can then be calculated according to the Stokes-Einstein equation: $D = k_B T/6\pi\eta R_h$, where k_B is Boltzmann's constant, T is the absolute temperature and η is the shear viscosity of the solvent.

All solutions for light scattering experiments were prepared using deionized water obtained with Easy-Pure II RF system (Barnstead). The buffer was placed in a cylindrical cell with a diameter of 6.3 mm and incubated for 5 min at 25°C. Cells with stoppers were used for incubation at high temperature to avoid evaporation. The aggregation process was initiated by the addition of an aliquot of protein to a final volume of 0.5 ml. When studying the kinetics of aggregation of proteins, the scattering light was collected at 90° scattering angle.

Dimensions of the fast thermostat used for heating of the protein solution were the following: 15 mm (diameter)×40 mm (height). Temperature gradients in such a thermostat are less than 0.1 degree. Notice that large temperature gradients in the sample cell would result in a developed convection of fluid. The correlation function of light, scattered on the convective flow, is quite different from the exponential correlation function in case of light scattering on diffusing particles. That is why we can reliably estimate the appearance of temperature gradients by analyzing measured correlation functions.

Calculations

OriginPro 8.0 SR0 software (OriginLab Corporation, USA) and Scientist software (MicroMath, Inc., USA) were used for the calculations. To characterize the degree of agreement between the experimental data and calculated values, we used the coefficient of determination R^2 (without considering the statistical weight of the measurement results) [34]:

$$R^2 = \frac{\sum_{i=1}^{i=n}\left(Y_i^{obs} - \overline{Y}^{obs}\right)^2 - \sum_{i=1}^{i=n}\left(Y_i^{obs} - Y_i^{calc}\right)^2}{\sum_{i=1}^{i=n}\left(Y_i^{obs} - \overline{Y}^{obs}\right)^2}, \qquad (5)$$

where $\overline{Y}^{obs} = \frac{1}{n}\sum_{i=1}^{i=n} Y_i$ is the average of the experimental data (Y_i^{obs}), Y^{calc} is the theoretically calculated value of the function Y and n is the number of measurements.

Results and Discussion

Turbidimetric Registration of Phb Aggregation

Thermal aggregation of Ph*b* was studied in the regime wherein temperature was elevated with a constant rate (1°C/min). Fig. 1A

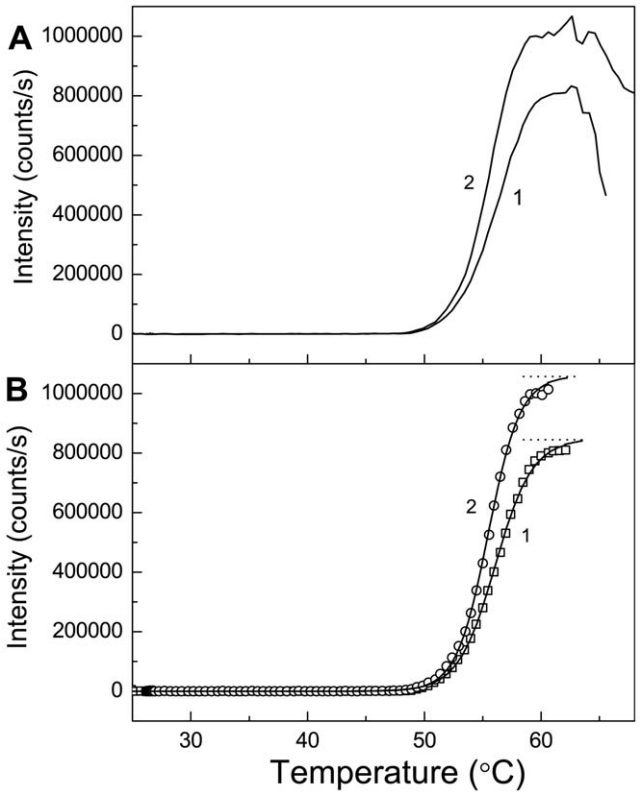

Figure 1. The dependences of the light scattering intensity at 632.8 nm on temperature for thermal aggregation of Ph*b* registered in the regime of heating with a constant rate (1°C/min). Conditions: 0.08 M Hepes-buffer, pH 6.8, containing 0.1 M NaCl. (**A**) The original experimental dependences. The Ph*b* concentrations were as follows: (1) 0.95 and (2) 1.9 mg/ml. (**B**) The results of fitting the experimental curves to Eq. (1). Points are the experimental data. The solid curves are calculated from Eq. (1). The dotted horizontal lines correspond to the limiting values of the light scattering intensity (I_{lim}).
doi:10.1371/journal.pone.0022154.g001

shows the dependences of the light scattering intensity on temperature for aggregation of Ph*b* at concentrations of 0.95 and 1.9 mg/ml (curves 1 and 2, respectively). When the temperature is elevated, the light scattering intensity reaches the limiting value. The decrease in the light scattering intensity at rather high temperatures is due to precipitation of the large-sized aggregates. Fig. 1B demonstrates the results of fitting Eq. (1) to the experimental data. The following values of parameters were established: $I_{lim} = (0.84 \pm 0.01) \cdot 10^6$ counts/s, $T_{agg} = 56.1 \pm 0.1$, $B = 1.57 \pm 0.02$ ($R^2 = 0.999$) at the Ph*b* concentration of 0.95 mg/ml and $I_{lim} = (1.05 \pm 0.01) \cdot 10^6$ counts/s, $T_{agg} = 55.5 \pm 0.1$, $B = 1.34 \pm 0.02$ ($R^2 = 0.999$) at the Ph*b* concentration of 1.9 mg/ml.

Denaturation of Ph*b* Registered by DSC and Comparison of the Turbidimetric and Calorimetric Data

When studying thermal aggregation of Ph*b*, we should take into account that the initial stage of the general process of aggregation is the stage of protein denaturation. To characterize Ph*b* denaturation, we used DSC. Fig. 2 shows DSC profiles obtained at the Ph*b* concentrations of 0.95 and 1.9 mg/ml (curves 1 and 2, respectively). The heating rate was 1°C/min. The increase in the Ph*b* concentration from 0.95 to 1.9 mg/ml results in the displacement of the maximum on the DSC profiles (T_m) from 53.7±0.1 to 54.2±0.1°C. This change in the shape of the DSC

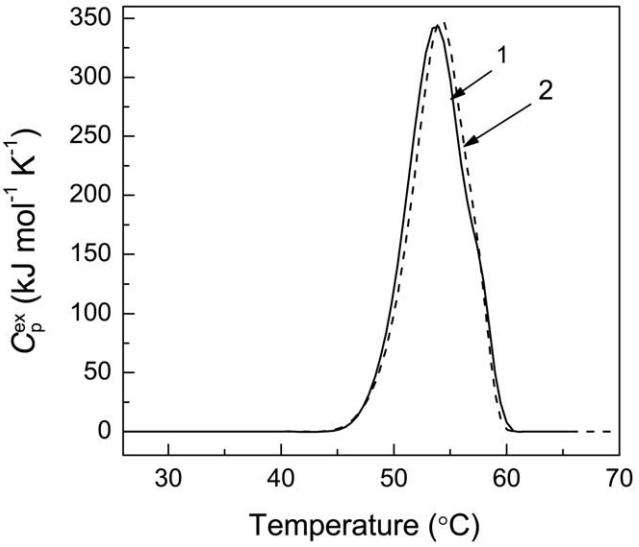

Figure 2. Thermal denaturation of Ph*b* (0.08 M Hepes-buffer, pH 6.8, containing 0.1 M NaCl). The dependences of the excess heat capacity (C_p^{ex}) on temperature, obtained at the following concentrations of Ph*b*: (1) 0.95 and (2) 1.9 mg/ml. C_p^{ex} was calculated per dimer of Ph*b* with the molecular mass of 194.8 kDa. The heating rate was 1°C/min.
doi:10.1371/journal.pone.0022154.g002

profile with variation of the Ph*b* concentration agrees with the dissociative mechanism of thermal denaturation of Ph*b* [10].

When a definite temperature has been achieved, the portion of the protein denatured by this temperature may be calculated from the area under the part of the DSC profile limited at this temperature (Q). If we know the area under the whole C_p^{ex} versus temperature profile (Q_{total}), the portion of denatured protein (γ_{den}) is equal to the Q/Q_{total} ratio. Fig. 3 shows the relationships between the light scattering intensity registered in the course of

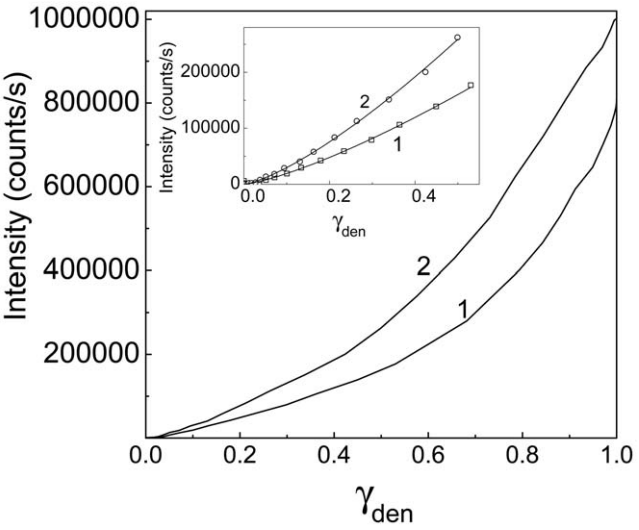

Figure 3. The relationships between the increment of the light scattering intensity accompanying Ph*b* aggregation and the portion of the denatured Ph*b* (γ_{den}) calculated from the DSC data. Ph*b* concentrations were as follows: (1) 0.95 and (2) 1.9 mg/ml. The inset shows the initial parts of the curves. Points are the experimental data. The solid curves are calculated from Eq. (6).
doi:10.1371/journal.pone.0022154.g003

Ph*b* aggregation and the γ_{den} value at two concentrations of Ph*b*. It can be seen that the increase in the light scattering intensity (I) is not a linear function of γ_{den}. Thus, in the case of thermal aggregation of Ph*b* the increment of the light scattering intensity cannot be considered as a direct measure of the degree of protein denaturation. It should be noted that in some cases a linear proportionality between the increase in the light scattering intensity and the degree of protein denaturation is really fulfilled. This, for example, was demonstrated by us for thermal aggregation of GAPDH [35].

The analysis of the relationship between the increment of the light scattering intensity (I) and the portion of the denatured Ph*b* presented in Fig. 3 showed that at $\gamma_{den}<0.5$ the I value was a power function of γ_{den}:

$$I = K\,\gamma_{den}^{N}. \qquad (6)$$

The following values of parameters K and N were found: $K=(4.0\pm0.1)\cdot10^5$ counts/s and $N=1.32\pm0.02$ ($R^2=0.999$) at the Ph*b* concentration of 0.95 mg/ml and $K=(6.6\pm0.1)\cdot10^5$ counts/s and $N=1.34\pm0.02$ ($R^2=0.999$) at the Ph*b* concentration of 1.9 mg/ml.

When comparing calorimetric and turbidimetric data obtained in the regime of heating with a constant rate, we should take into account the following features of the temperature dependences of excess heat capacity and the light scattering intensity. There is no threshold temperature on the DSC profile. The dependence of excess heat capacity on temperature asymptotically approaches zero level with decreasing temperature. The lower the temperature, the lower is the amount of the denatured protein accumulated to the moment when the given temperature has been achieved. On the contrary, an initial increase in the light scattering intensity is registered at definite temperature designated as T_0. According to the mechanism of thermal aggregation of proteins proposed in our works [12,23,35–37], the initial increase in the light scattering intensity corresponds to the moment of the origination of the start aggregates. The formation of the start aggregates proceeds on the all-or-none principle. The intermediate states between native enzyme forms (or denatured protein molecules) and start aggregates have not been detected.

Analysis of the Initial Parts of the Dependences of the Light Scattering Intensity on Temperature

In the present work the focus is concentrated on the initial parts of the dependences of the light scattering intensity on temperature. Fig. 4A shows the influence of the protein concentration on the initial parts of the kinetic curves of aggregation of Ph*b* heated with a constant rate of 1°C/min. The Ph*b* concentration was varied in the interval from 0.1 to 1.5 mg/ml. The experimental curves are satisfactorily described by the Eq. (4). The R^2 values lie in the range from 0.995 at [Ph*b*] = 0.1 mg/ml to 0.990 at [Ph*b*] = 1.5 mg/ml. The calculated values of parameters T_0 and K_{agg} are represented in Fig. 4B and C as a function of the Ph*b* concentration. Parameter T_0, characterizing the temperature at which the light scattering intensity begins to increase, decreases monotonously with increasing the concentration of Ph*b* (Fig. 4B).

When interpreting the dependence of parameter K_{agg} characterizing the rate of aggregation on the Ph*b* concentration, we should be aware that this dependence can not be used for estimation of the order of aggregation with respect to the protein because the K_{agg} values on the K_{agg} versus the Ph*b* concentration plot correspond, in fact, to different temperatures. It is of interest that at the Ph*b* concentration higher than 0.5 mg/ml parameter

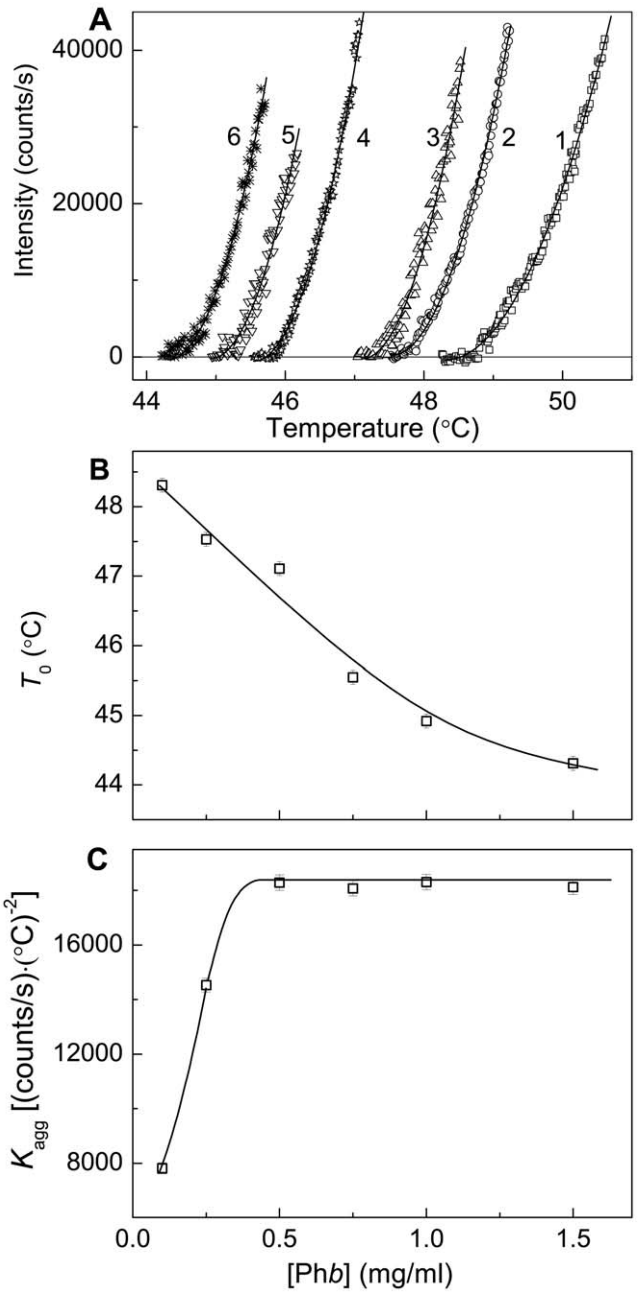

Figure 4. Analysis of the kinetics of Ph*b* aggregation registered in the regime of heating at the rate of 1°C/min. (**A**) The initial parts of the dependences of the light scattering intensity on temperature obtained at the following concentrations of Ph*b*: (1) 0.1, (2) 0.25, (3) 0.5, (4) 0.75, (5) 1.0 and (6) 1.5 mg/ml. Points are the experimental data. The solid curves were calculated from Eq. (4). (**B** and **C**) The dependences of parameters T_0 and K_{agg} calculated from Eq. (4) on the Ph*b* concentration, respectively.
doi:10.1371/journal.pone.0022154.g004

K_{agg} is a constant value, which is independent of the protein concentration (Fig. 4C). When the Ph*b* concentration is lower than 0.5 mg/ml, decreasing the protein concentration results in the decrease in the K_{agg} value.

It was of interest to investigate whether the character of the dependences of parameters T_0 and K_{agg} on the protein concentration observed for Ph*b* remains the same for other proteins. Fig. 5 shows the analysis of the initial parts of the

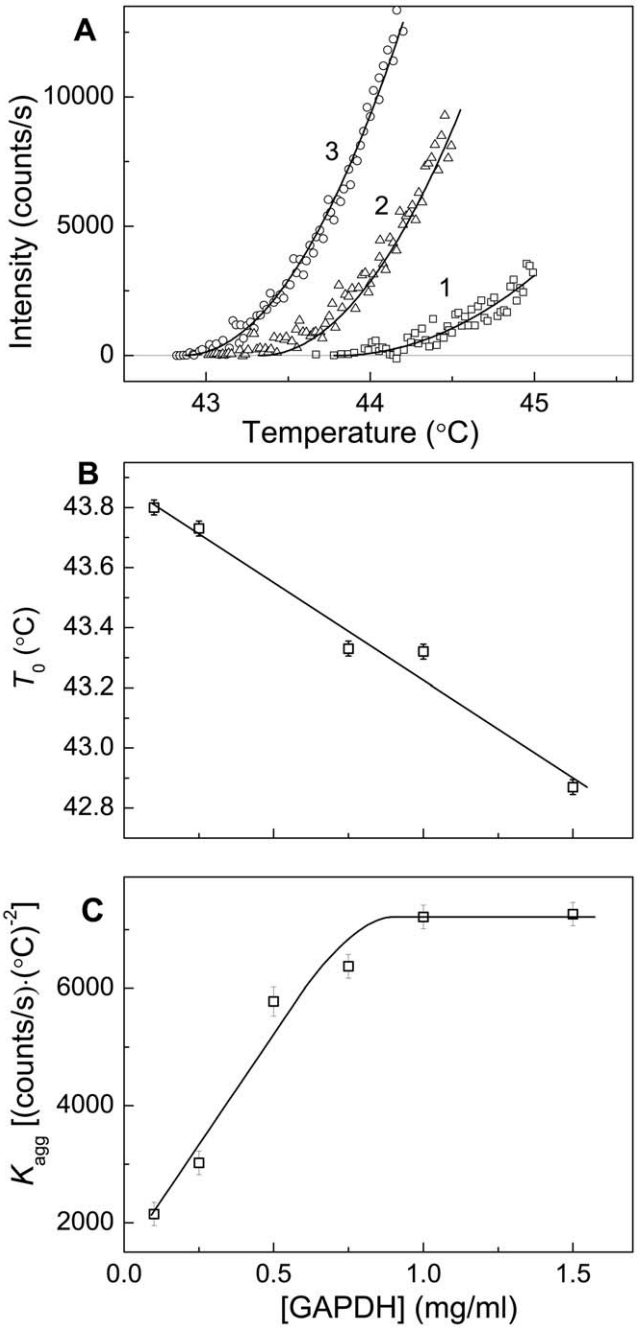

Figure 5. Analysis of the kinetics of GAPDH aggregation registered in the regime of heating at the rate of 1°C/min (10 mM Na-phosphate buffer, pH 7.5, containing 0.1 M NaCl). (**A**) The initial parts of the dependences of the light scattering intensity on temperature obtained at the following concentrations of GAPDH: (1) 0.1, (2) 0.75 and (3) 1.5 mg/ml. Points are the experimental data. The solid curves were calculated from Eq. (4). (**B** and **C**) The dependences of parameters T_0 and K_{agg} calculated from Eq. (4) on the GAPDH concentration, respectively.
doi:10.1371/journal.pone.0022154.g005

dependences of the light scattering intensity on temperature for thermal aggregation of GAPDH. The protein concentration was varied in the interval from 0.1 to 1.5 mg/ml. As an example, the kinetics of GAPDH aggregation at the protein concentrations of 0.1, 0.75 and 1.5 mg/ml and the results of fitting the experimental data to Eq. (4) are represented in Fig. 5A. The R^2 values for approximation of the curves shown in Fig. 5A by Eq. (4) were found to be 0.881, 0.974 and 0.990 at the GAPDH concentrations of 0.1, 0.75 and 1.5 mg/ml, respectively. The calculated values of parameters T_0 and K_{agg} are represented in Fig. 5B and C as a function of the GAPDH concentration. As in the case of Ph*b*, parameter T_0 decreases monotonously with increasing the GAPDH concentration and parameter K_{agg} reaches a constant value at rather high protein concentrations.

Fig. 6A demonstrates the applicability of Eq. (4) for the description of the initial parts of the dependences of the light scattering intensity on temperature obtained for aggregation of CK at various concentrations of the protein. The R^2 values for approximation of these dependences by Eq. (4) lie in the range from 0.846 at [CK] = 0.25 mg/ml to 0.985 at [CK] = 1.5 mg/ml. When the concentration of CK increases from 0.1 to 1.5 mg/ml, the T_0 value decreases monotonously from 45.2 to 40.7°C (Fig. 6B). The value of parameter K_{agg} increases with increasing the CK concentration (Fig. 6C). There is no tendency for K_{agg} to level off at high concentrations of the protein.

Sabbaghian et al. [11] showed that interaction of small molecules (coenzymes, allosteric effectors) with the bovine liver GDH resulted in profound changes in the extent of its thermal aggregation. It was of interest to study thermal aggregation of GDH in the regime of elevating the temperature with a constant rate. The initial parts of the dependences of the light scattering intensity on temperature obtained at various concentrations of GDH were analyzed using Eq. (4) (Fig. 7A), and the corresponding values of parameters T_0 and K_{agg} were calculated. The R^2 values for approximation of the curves presented in Fig. 7A by Eq. (4) were found to be 0.990. The value of parameter T_0 remains practically constant with variation of the GDH concentration (Fig. 7B). The average value of T_0 is equal to 34.8±0.2°C. As it can be seen from Fig. 7C, parameter K_{agg} increases monotonously with increasing the protein concentration.

We have also analyzed the dependences of the light scattering intensity on temperature for aggregation of human interleukin 1-β presented by Chrunyk et al. [38]. These dependences were obtained at various protein concentrations. The heating rate was 0.5°C/min. The following values of parameters of Eq. (4) were found: T_0 = 50.0±0.1, 48.4±0.1 and 47.5±0.1°C, K_{agg} = 317±15, 1130±50 and 2200±100 (°C)$^{-2}$ for the interleukin 1-β concentration equal to 1, 2 and 4 mg/ml, respectively. The R^2 values for approximation of the experimental curves by Eq. (4) were equal to 0.965, 0.913 and 0.846 at the interleukin 1-β concentration of 1, 2 and 4 mg/ml, respectively. Thus, the enhancement of the interleukin 1-β concentration results in the diminishing of the value of parameter T_0 and the increase in the K_{agg} value. It is worthy of mention that to characterize the temperature aggregation Chrunyk et al. [39] proposed to use a temperature corresponding to the length cut off on the temperature axis by the straight line, which is a continuation of the linear part of the dependence of the light scattering intensity on temperature reachable at the inflexion point.

In the work of Raibekas [40] the dependences of the light scattering intensity on temperature for aggregation of interleukin-1 receptor antagonist (IL-1ra) are represented in the coordinates $\{I/I_{lim}; T\}$. The heating rate was 1°C/min. The dependences I/I_{lim} on temperature were obtained at various concentrations of IL-1ra and characterized by parameter T_{agg} corresponding to the level $I/I_{lim} = 0.5$. In the interval concentrations of IL-1ra from 1 to 10 mg/ml parameter T_{agg} decreases by 5.3°C, namely from 56.4 to 51.1°C ($\Delta T_{agg} = 5.3$°C). We have analyzed the dependences of I/I_{lim} on temperature using an equation, which is a modification of Eq. (4):

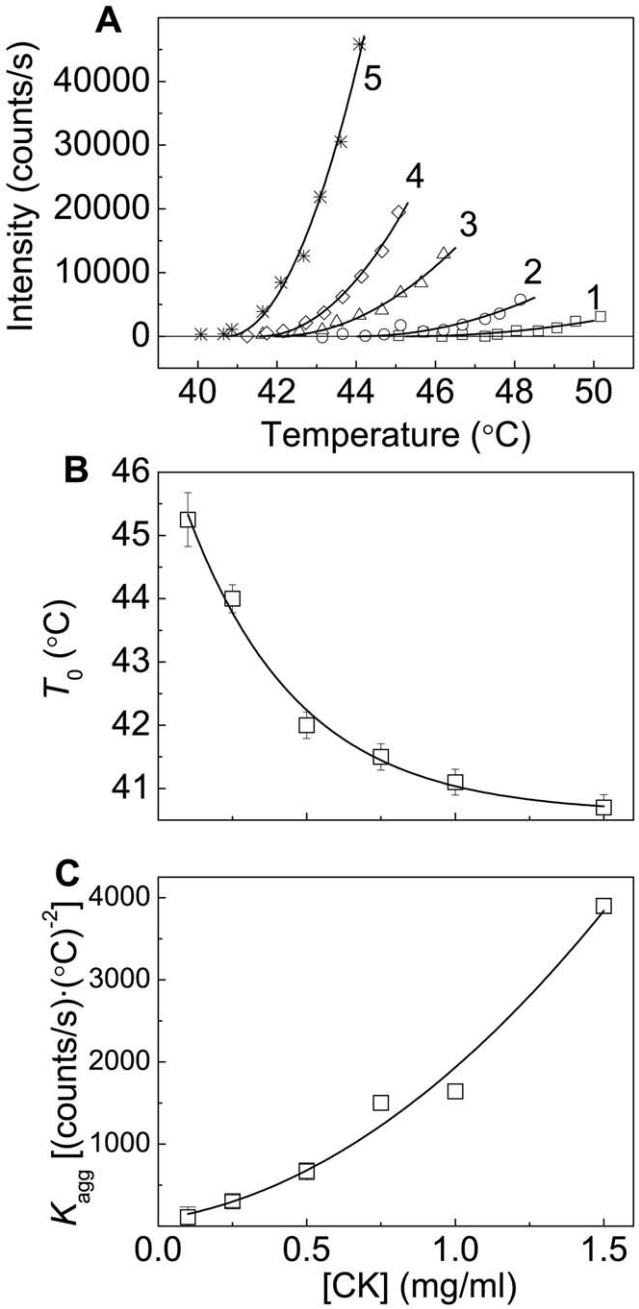

Figure 6. Analysis of the kinetics of CK aggregation registered in the regime of heating at the rate of 1°C/min (30 mM Hepes–NaOH buffer, pH 8.0, containing 0.1 M NaCl). (**A**) The initial parts of the dependences of the light scattering intensity on temperature obtained at the following CK concentrations: (1) 0.1, (2) 0.25, (3) 0.5, (4) 0.75 and (5) 1.5 mg/ml. Points are the experimental data. The solid curves were calculated from Eq. (4). (**B** and **C**) The dependences of parameters T_0 and K_{agg} calculated from Eq. (4) on the CK concentration, respectively.
doi:10.1371/journal.pone.0022154.g006

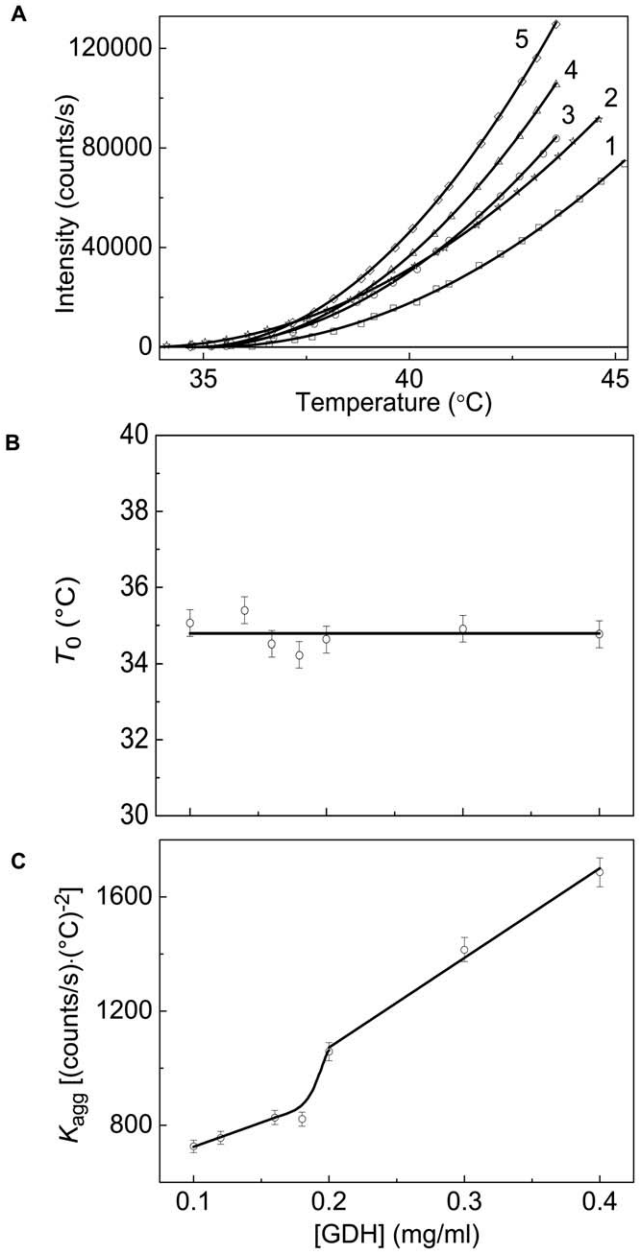

Figure 7. Analysis of the kinetics of GDH aggregation registered in the regime of heating at the rate of 1°C/min (0.1 M Na-phosphate buffer, pH 7.6). (**A**) The initial parts of the dependences of the light scattering intensity on temperature obtained at the following concentrations of GDH: (1) 0.1, (2) 0.12, (3) 0.2, (4) 0.3 and (5) 0.4 mg/ml. Points are the experimental data. The solid curves were calculated from Eq. (4). (**B** and **C**) The dependences of parameters T_0 and K_{agg} calculated from Eq. (4) on the GDH concentration, respectively.
doi:10.1371/journal.pone.0022154.g007

$$I/I_{\lim} = K_{agg}^{rel}(T - T_0)^2. \quad (T > T_0) \qquad (7)$$

In this equation K_{agg}^{rel} is a constant. The change in the T_0 value characterizes the displacement of the dependence of $I/I_{\lim}$ on temperature along the abscissa axis, whereas parameter K_{agg}^{rel} characterizes the steepness of the initial part of the dependence of $I/I_{\lim}$ on T. The following values of parameters of Eq. (7) were found: $T_0 = 53.7 \pm 0.1$°C and $K_{agg}^{rel} = 0.080 \pm 0.002$ $(°C)^{-2}$ ($R^2 = 0.994$) at [IL-1ra] = 1 mg/ml and $T_0 = 47.3 \pm 0.1$°C and $K_{agg}^{rel} = 0.044 \pm 0.001$ $(°C)^{-2}$ ($R^2 = 0.997$) at [IL-1ra] = 10 mg/ml. If one assumes that the $I_{\lim}$ value is strictly proportional to the

protein concentration, the calculations show that K_{agg} should increase by a factor of 5.5 when the IL-1ra concentration increases from 1 to 10 mg/ml. The displacement of the dependence of I/I_{lim} on temperature in this concentration interval was characterized by the change in parameter T_0, and ΔT_0 was equal to 6.4°C. This value is less than ΔT_{agg} (5.3°C). The discrepancy between the values of ΔT_0 and ΔT_{agg} is explained by the lesser steepness of the initial part of the dependence of I/I_{lim} on temperature and, consequently, the lesser slope of this dependence in the inflexion point at [IL-1ra] = 10 mg/ml.

Thus, the quantitative analysis of the initial parts of the dependences of the light scattering intensity on temperature using Eq. (4) allows us to estimate the threshold temperature T_0 and parameter K_{agg}, which may be considered as a measure of the rate of aggregation. Parameter T_0 has a clear physical sense. When the measurement of the light scattering intensity is used for registration of protein aggregation, the initial increment of the light scattering intensity corresponds to the instant of the formation of the start aggregates containing hundreds of denatured protein molecules [25,26]. The value of parameter T_0 is a function of the protein concentration and, as a rule, decreases with increasing the protein concentration. As it could be expected, the value of parameter K_{agg} characterizing the aggregation rate tends to grow as the protein concentration increases. In some cases the leveling off for the K_{agg} value is observed at rather high concentrations of the protein, as with Ph*b* and GAPDH. Such unexpected decrease in the growth of the aggregation rate with increasing protein concentration may have a simple explanation. When the protein concentration increases, the diminishing of the initial aggregation temperature (T_0) occurs, and, consequently, the initial rate of aggregation is measured in the region of lower temperatures.

Two parameters we proposed to characterize the temperature dependence of the light scattering intensity (T_0 and K_{agg}) provide more detailed information on the character of protein aggregation than parameter T_{agg}. Really, the value of parameter T_{agg} is determined by two factors, namely the threshold temperature T_0 and the steepness of the initial part of the dependence of the light scattering intensity on temperature expressed by parameter K_{agg} (or parameter K_{agg}^{rel}).

Apart from the protein concentration there is another factor affecting the shape on the light scattering intensity versus temperature plot, namely the heating rate. One could expect that an increase in the heating rate would result in the displacement of the dependence of the light scattering intensity on temperature towards higher temperatures. Actually, such a picture was observed for aggregation of α-amylase from *Bacillus amyloliquefaciens* (BAA). Duy and Fitter [41] studied aggregation of BAA at various values of the heating rate (v). The protein concentration was 50 μg/ml. The experimental data were represented by the coordinates $\{I/I_{lim}; T\}$. An analysis of the dependences of I/I_{lim} on temperature based on Eq. (7) gives the following values of parameters: $T_0 = 74.0 \pm 0.1$°C and $K_{agg}^{rel} = 0.0052 \pm 0.0002$ $(°C)^{-2}$ ($R^2 = 0.964$) at $v = 0.1$°C/min and $T_0 = 79.8 \pm 0.1$°C and $K_{agg}^{rel} = 0.0070 \pm 0.0005$ $(°C)^{-2}$ ($R^2 = 0.949$) at $v = 1.0$°C/min. Thus the enhancement of the heating rate from 0.1 to 1.0°C/min results in the displacement of the dependence of the light scattering intensity on temperature along the abscissa axis by 5.8°C towards higher temperatures. The change in the steepness of the initial part of the dependence of the light scattering intensity on temperature is not marked. Parameter K_{agg}^{rel} increases by a factor of 1.35, when the heating rate is changed from 0.1 to 1.0°C/min. It should be noted that the change in the value of parameter T_{agg} corresponding to the level $I/I_{lim} = 0.5$ in this interval of the heating rates was equal to 3.3°C. Consequently, ΔT_{agg} is less than ΔT_0. Apart from the light scattering measurements the authors studied thermal unfolding of BAA using intrinsic fluorescence spectroscopy. Unfolding transitions were analyzed in terms of wavelength shifts of the emission peak and by calculating the peak ratios of intensities as measured at 330 nm and 350 nm (excitation wavelengths of 280 and 295 nm were applied). It was shown that for both heating rates (0.1 and 1.0°C/min) aggregation that was characterized by the normalized change in the light scattering intensity appeared rather concurrent with respect to the unfolding transition as obtained from tryptophan fluorescence.

Estimation of the Size of Protein Aggregates

Consider what additional information on the aggregation process studied in the regime of heating with a constant rate may be obtained from the measurements of the size of the protein aggregates. Fig. 8A shows the initial parts of the dependences of the hydrodynamic radius (R_h) of the protein aggregates on temperature obtained for GAPDH aggregation at various concentrations of the protein. These dependences are linear, and the following equation was used for their analysis [24,25]:

$$R_h = R_{h,0}\left[1 + \frac{1}{\Delta T_{2R}}(T - T_0)\right]. \quad (T > T_0) \qquad (8)$$

In this equation $R_{h,0}$ is the hydrodynamic radius of the start aggregates, T_0 is the temperature at which the start aggregates appear and ΔT_{2R} is the temperature interval over which the hydrodynamic radius of the protein aggregates increases from $R_{h,0}$ to $2R_{h,0}$. The reciprocal value of parameter ΔT_{2R} is a measure of the aggregation rate. The higher the $1/\Delta T_{2R}$ value, the higher is the aggregation rate. Taking T_0 in this equation to be identical to parameter T_0 in Eq. (4), we can calculate other parameters, namely $R_{h,0}$ and ΔT_{2R}. As it can be seen from Fig. 8B, the marked decrease in the $R_{h,0}$ value occurs with increasing GAPDH concentration (from 64±3 nm at [GAPDH] = 0.1 mg/ml to 14±3 nm at [GAPDH] = 1.5 mg/ml). Such a decrease in the $R_{h,0}$ value is accompanied by the increase in the rate of aggregation expressed by the reciprocal value of parameter ΔT_{2R} (Fig. 8C).

Fig. 9A shows the initial parts of the dependences of the hydrodynamic radius of protein aggregates on temperature obtained for CK aggregation at various concentrations of the protein. These dependences are exponential, and the following equation was used for their analysis [24–26]:

$$R_h = R_{h,0}\exp\left[\frac{\ln 2}{\Delta T_{2R}}(T - T_0)\right]. \quad (T > T_0) \qquad (9)$$

In this equation ΔT_{2R} is the temperature interval over which the hydrodynamic radius is doubled. When the concentration of the protein increases, a slight diminishing of the $R_{h,0}$ value takes place (from 44±2 nm at [CK] = 0.1 mg/ml to 34±2 nm at [CK] = 1.5 mg/ml) with simultaneous increase in the $1/\Delta T_{2R}$ value (Fig. 9B and C).

As is with CK, the initial parts of the dependences of the hydrodynamic radius of protein aggregates on temperature obtained for GDH aggregation at various concentrations of the protein are exponential (Fig. 10A). The values of parameters $R_{h,0}$ and $1/\Delta T_{2R}$ as a function of the GDH concentration are represented in Fig. 10B and C. The increase in the GDH concentration results in the diminishing of the $R_{h,0}$ value with simultaneous increase in the $1/\Delta T_{2R}$ value.

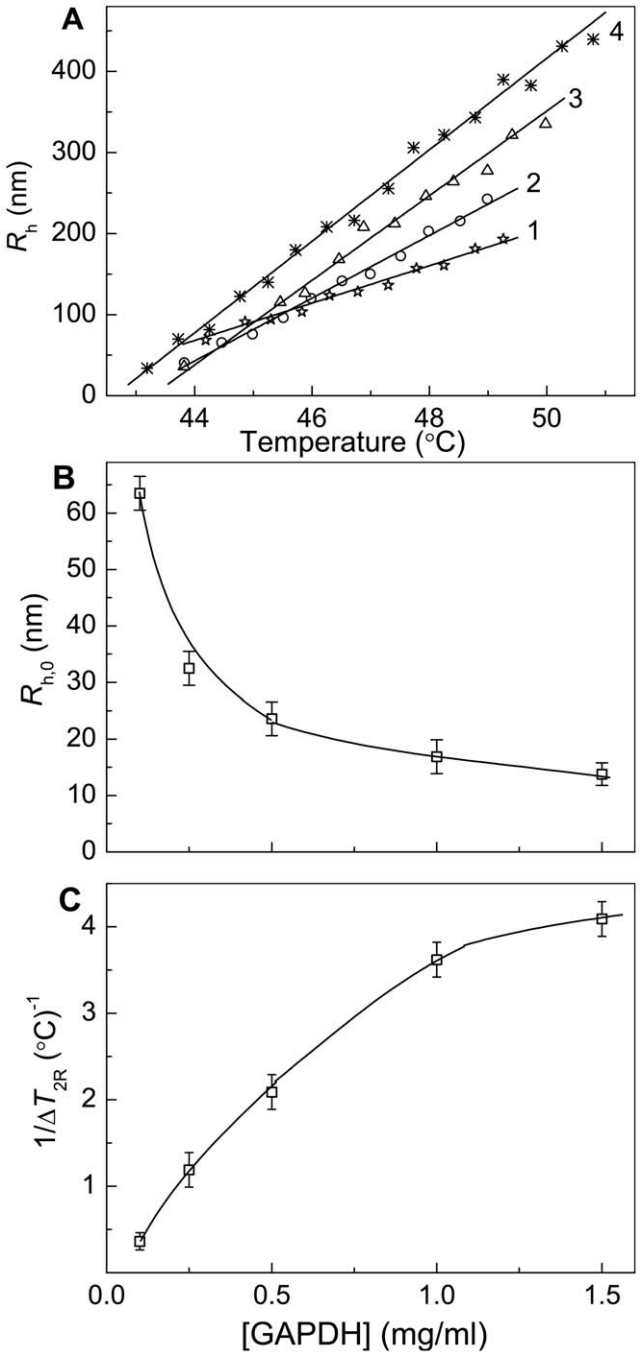

Figure 8. Estimation of the size of the protein aggregates formed in the course of GAPDH aggregation registered in the regime of heating at the rate of 1°C/min (10 mM Na-phosphate buffer, pH 7.5, containing 0.1 M NaCl). (**A**) The initial parts of the dependences of the hydrodynamic radius (R_h) of the protein aggregates on temperature obtained at the following GAPDH concentrations: (1) 0.1, (2) 0.25, (3) 0.5 and (4) 1.5 mg/ml. (**B** and **C**) The dependences of parameter $R_{h,0}$ and the reciprocal value of parameter ΔT_{2R} calculated from Eq. (8) on the GAPDH concentration, respectively.
doi:10.1371/journal.pone.0022154.g008

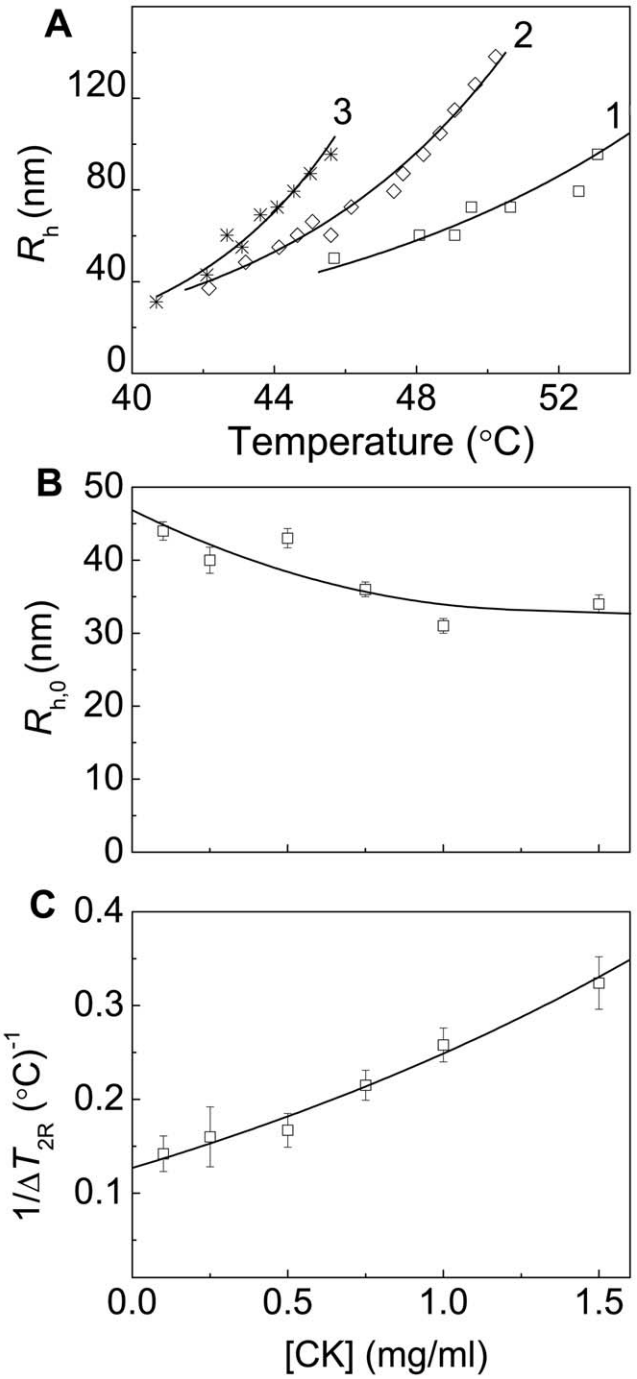

Figure 9. Estimation of the size of the protein aggregates formed in the course of CK aggregation registered in the regime of heating at the rate of 1°C/min (30 mM Hepes–NaOH buffer, pH 8.0, containing 0.1 M NaCl). (**A**) The initial parts of the dependences of the hydrodynamic radius (R_h) of the protein aggregates on temperature obtained at the following CK concentrations: (1) 0.1, (2) 0.75 and (3) 1.5 mg/ml. (**B** and **C**) The dependences of parameter $R_{h,0}$ and the reciprocal value of parameter ΔT_{2R} calculated from Eq. (9) on the GAPDH concentration, respectively.
doi:10.1371/journal.pone.0022154.g009

The following explanation can be proposed for the decrease in parameter T_0 with increasing the protein concentration (Fig. 4–6). The increase in the protein concentration favors nucleation and further formation of start aggregates. Therefore one may expect that the temperature corresponding to the moment of origination of the start aggregates will decrease with increasing the protein concentration. This picture resembles the well-known phenomenon of the decrease in the duration of the lag period on the kinetic curves of aggregation registered at a fixed temperature when the

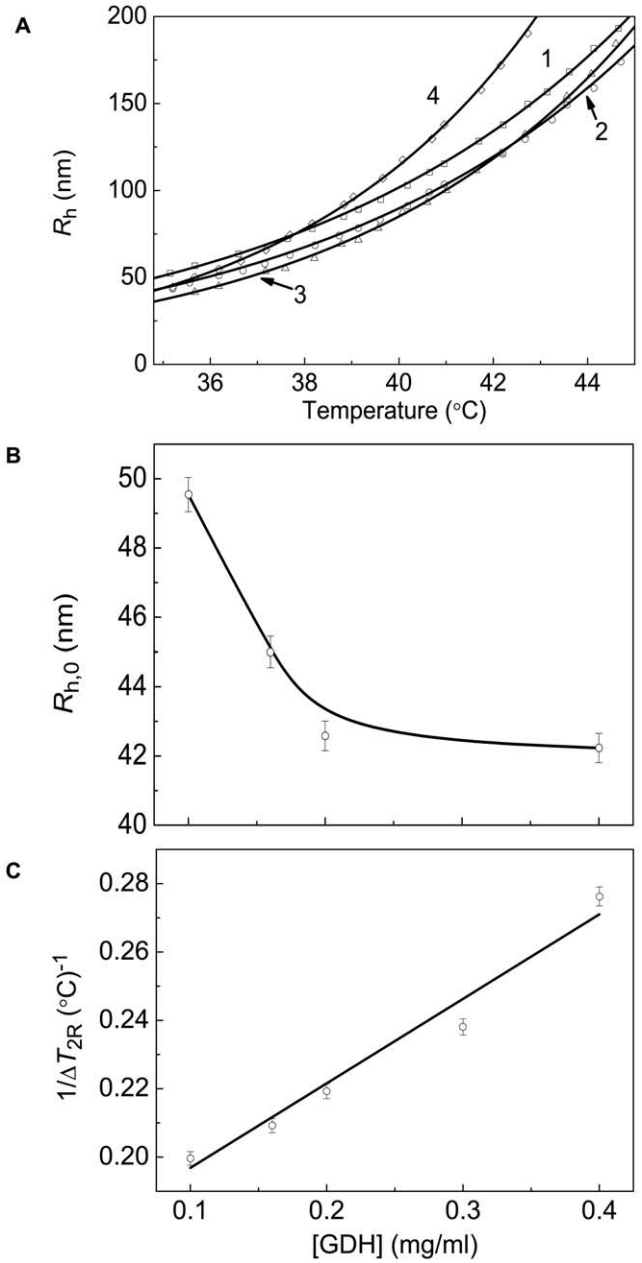

Figure 10. Estimation of the size of the protein aggregates formed in the course of GDH aggregation registered in the regime of heating at the rate of 1°C/min (0.1 M Na-phosphate buffer, pH 7.6). (**A**) The initial parts of the dependences of the hydrodynamic radius (*R*h) of the protein aggregates on temperature obtained at the following GDH concentrations: (1) 0.1, (2) 0.2, (3) 0.3 and (4) 0.4 mg/ml. (**B** and **C**) The dependences of parameter $R_{h,0}$ and the reciprocal value of parameter ΔT_{2R} calculated from Eq. (9) on the GDH concentration, respectively.
doi:10.1371/journal.pone.0022154.g010

concentration of the model protein increases (see, for example [17,26,35,36]).

We can interpret the linear character of the dependence of the hydrodynamic radius of protein aggregates on temperature observed for GAPDH as an indication of the fulfillment of the diffusion-limited aggregation regime, wherein the rate of aggregation is limited by diffusion of the colliding particles (the so-called regime of diffusion-limited cluster–cluster aggregation) [24,25]. In other words, the sticking probability for the colliding particles for this regime of aggregation is equal to unity. We interpret the exponential character of the dependence of the hydrodynamic radius of the protein aggregates on temperature observed for CK and GDH as an indication for the fulfillment of the regime of reaction-limited cluster-cluster aggregation wherein the sticking probability for the colliding particles is lower than unity [24–26].

Consider the differences between the model of protein aggregation used in the present work and models proposed by other investigators. A general model of protein aggregation was recently elaborated by Li and Roberts [42]. This model takes into account the conformational transition of monomers between folded and unfolded states, nucleation of the smallest aggregate species, growth of aggregates via chain polymerization and aggregate growth due to aggregate-aggregate association. When studying the kinetics of thermal aggregation of proteins by dynamic light scattering, we observed that at the moment of time when the initial increment in the light scattering intensity is observed, protein aggregates containing hundreds of denatured protein molecules are registered. These primary aggregates were called the start aggregates. We could not detect intermediate states between the non-aggregated form of the protein and the start aggregates. Thus we infer that the formation of the start aggregates proceeds on the all-or-none principle. This pattern was demonstrated for thermal aggregation of β_L-crystallin from bovine lens [12,37], GAPDH from rabbit skeletal muscle [6,23,35,37,43], yeast alcohol dehydrogenase I [26,37], tobacco mosaic virus coat protein [37,44], Ph*b* from rabbit skeletal muscle [5,23,29, 37,43,45], aspartate aminotransferase from pig heart mitochondria [46] and creatine kinase from rabbit skeletal muscle [7]. On the basis of these experimental data a new model of protein aggregation was proposed [12,23,36,37]. According to this model nuclei are assembled rather quickly in the start aggregates and further growth of aggregates is due to sticking of the start aggregates and aggregates of higher order. It was demonstrated that the size of the start aggregates is independent of the concentration of the protein involved in aggregation. This fact allowed us to draw an analogy between the formation of the start aggregates and micelle formation. In the latter case the micelles of a definite size are formed when the critical micelle concentration is achieved. Such an analogy offers an explanation of why the formation of start aggregates proceeds according to the all-or-none principle.

The idea on the formation of primary aggregates in the course of protein aggregation was also used by Durand and coworkers.When studying thermal aggregation of β-lactoglobulin at pH 7.0 by size exclusion chromatography, Durand et al. [47–51] showed that there was a clear separation between a narrow peak that corresponded to residual native protein and a broad peak that corresponded to the aggregates. This observation implied that the aggregates of the minimum size contained many monomers and that no or very few stable oligomers were formed. The authors supposed that the first stage of thermal aggregation of β-lactoglobulin was the step of the formation of ''primary aggregates''.

Shiraki and coworkers [52] studied heat-induced aggregation of lysozyme at around the isoelectric point. Dynamic light scattering and transmission electron microscopy revealed that aggregation occurred in a two-step process: formation of start aggregates, followed by further growth mediated by their sticking with diffusion-limited cluster-cluster aggregation.

Recent investigations of dithiothreitol-induced aggregation of alpha-lactalbumin and insulin using dynamic light scattering convincingly demonstrate that the aggregation process

proceeds through the stage of formation of the start aggregates [53,54].

It is notable that according to present views the assembly of amyloid fibrils proceeds through the stage of the formation of protofibrils. Association of protofibrils results in the formation of fibrils and then clusters of fibrils and bundles [55,56]. It is evident that protofibrils are equivalent to the start aggregates in the case of aggregation producing amorphous aggregates (this analogy was discussed in Golub et al. [23]).

Screening of the Ligands Affecting Denaturation or Aggregation of Ph*b* and GDH on the Basis of the Data of the Aggregation Kinetics

Consider the use of this new approach to characterization of the aggregation rate for the quantitative estimation of the ability of various agents to suppress protein aggregation. Our investigations have shown that Ph*b* is a convenient model for testing the compounds affecting protein denaturation and aggregation [4,5,25,29,45,57–60]. Fig. 11 shows the effect of some agents on Ph*b* aggregation. The suppression of aggregation in the presence of 1 mM AMP is accompanied by the increase in the T_0 value from 47.2°C (curve 1; the control) to 51.4°C (curve 2; 1 mM AMP) and the decrease in parameter K_{agg} from $(1.83\pm0.02)\cdot10^5$ (curve 1) to $(1.20\pm0.02)\cdot10^5$ (counts/s)·(°C)$^{-2}$ (curve 2). Based on the data on kinetics of thermal inactivation of Ph*b* and DSC data [58,60], we can conclude that the anti-aggregation ability of allosteric activator AMP is due to the stabilization of the native Ph*b* molecule. The acceleration of Ph*b* aggregation in the presence of HP-β-CD (curve 3 in Fig. 11) is accompanied by the decrease in the T_0 value to 46.1°C and the increase in parameter K_{agg} to $(3.27\pm0.03)\cdot10^5$ (counts/s)·(°C)$^{-2}$. This action of HP-β-CD is caused by the destabilization of the Ph*b* molecule as a result of binding of HP-β-CD to the native form of the enzyme and early intermediates of Ph*b* unfolding as suggested by the data on the kinetics of thermal inactivation and DSC data [45]. It is known that osmolytes stabilize the protein structure [61–63]. Therefore, when testing the effect of osmolytes on protein aggregation, one can expect that osmolytes will reveal the protective action. Fig. 11 demonstrates that a markedly expressed retardation of thermal aggregation of Ph*b* is observed in the presence of 1 M TMAO. The T_0 value increases to 55.1°C and the K_{agg} value decreases to $(1.54\pm0.02)\cdot10^5$ (counts/s)·(°C)$^{-2}$ (curve 4). At last, it is of interest to discuss the effect of the agents of protein nature responsible for suppression of protein aggregation in the cell, namely small heat shock proteins. Meremyanin et al. [25,29] showed that α-crystallin, one of the representatives of small heat shock protein family, effectively hindered thermal aggregation of Ph*b*. Curve 5 in Fig. 11 presents an initial part of the dependence of the light scattering intensity on temperature for Ph*b* aggregation measured in the presence of α-crystallin at the concentration of 1 mg/ml. The protective action of α-crystallin is reflected in the increase in the T_0 value (to 52.6°C) and the marked decrease in the K_{agg} value (to $(0.27\pm0.01)\cdot10^5$ (counts/s)·(°C)$^{-2}$). The R^2 values for approximation of the curves 1–5 shown in Fig. 11 by Eq. (4) were found to be 0.981, 0.954, 0.987, 0.986 and 0.972, respectively. The values of parameters of T_0 and K_{agg} obtained during testing of the effect of various agents on Ph*b* aggregation are given in Table 1.

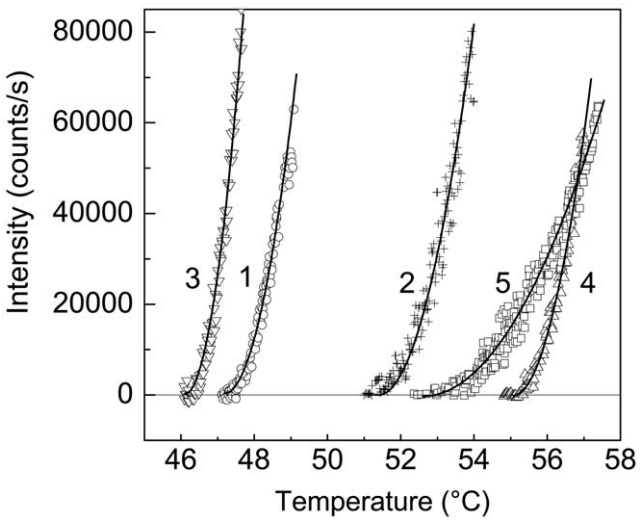

Figure 11. Effect of different agents on Ph*b* aggregation. The initial parts of the dependences of the light scattering intensity on temperature for aggregation of Ph*b* (0.5 mg/ml) in the presence of the following agents: (1) control, (2) 1 mM AMP, (3) 0.19 M HP-β-CD, (4) 1 M TMAO and (5) α-crystallin at the concentration of 1 mg/ml. Points are the experimental data. The solid curves were calculated from Eq. (4).
doi:10.1371/journal.pone.0022154.g011

Fig. 12 shows the effect of specific ligands (NADH, ADP, L-glutamate and L-leucine) on aggregation of GDH studied in the regime of heating with a constant rate. The values of parameters T_0 and K_{agg} are given in Table 2. The increase in parameter K_{agg} in the presence of 0.2 mM NADH means that NADH displays the destabilizing action on the enzyme. Judging from the K_{agg} values, the enhancement of GDH stability is observed in the presence of allosteric activators, ADP and L-leucine, and in the presence of substrate, L-glutamate. ADP (0.5 mM) eliminates the destabilizing effect of NADH (0.2 mM). NAD has no effect on GDH aggregation (see Table 2).

The effect of ADP on aggregation of GDH was studied in greater detail. Fig. 13A shows the initial parts of the dependences of the light scattering intensity on temperature obtained for GDH aggregation at various concentrations of ADP. The values of parameters T_0 and K_{agg} as a function of the ADP concentration are represented in Fig. 13B and C. A sharp increase in parameter T_0 is observed in the presence of 0.05 mM ADP, namely from 35.2°C at [ADP] = 0 to 38.7°C at [ADP] = 0.05 mM (Fig. 13B). The changes in parameter T_0 in the interval of ADP concentration from 0.05 to 0.5 mM are insignificant. The average value of T_0 in this interval of ADP concentrations is equal to 39.1 ± 0.2°C. A decrease in parameter T_0 is observed at the ADP concentrations higher than 0.5 mM. As it follows from Fig. 13C, the increase in ADP concentration is accompanied by the diminishing of parameter K_{agg}. The dependence of K_{agg} on ADP concentration in the interval 0.05–0.5 mM was analyzed using the following equation:

Table 1. Parameters of aggregation of Ph*b* (0.5 mg/ml) in the presence of different ligands (0.08 M Hepes-buffer, pH 6.8, containing 0.1 M NaCl).

Ligand	T_0 (°C)	K_{agg} [(counts/s)·(°C)$^{-2}$]
-	47.2±0.1	$(1.83\pm0.02)\cdot10^5$
AMP (1 mM)	51.4±0.1	$(1.20\pm0.02)\cdot10^5$
HP-β-CD (19 mM)	46.1±0.1	$(3.27\pm0.03)\cdot10^5$
TMAO (1 M)	55.1±0.1	$(1.54\pm0.02)\cdot10^5$
α-crystallin (1 mg/ml)	52.6±0.1	$(0.27\pm0.01)\cdot10^5$

doi:10.1371/journal.pone.0022154.t001

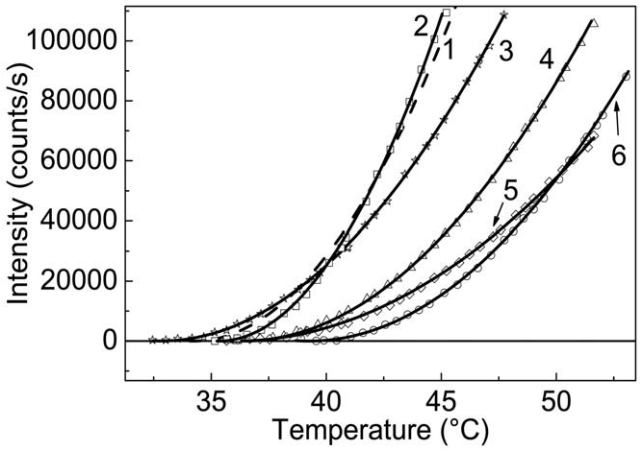

Figure 12. Effect of different agents on GDH aggregation. The initial parts of the dependences of the light scattering intensity on temperature for aggregation of GDH (0.12 mg/ml) in the presence of the following agents: (1) control; (2) 0.2 mM NADH; (3) 50 mM L-glutamate; (4) 0.2 mM NADH+0.5 mM ADP; (5) 50 mM L-leucine and (6) 0.5 mM ADP. Points are the experimental data. The solid curves were calculated from Eq. (4).
doi:10.1371/journal.pone.0022154.g012

$$K_{\mathrm{agg}} = \frac{K_{\mathrm{agg},0}}{(1+[\mathrm{ADP}]/K_{\mathrm{diss}})}, \qquad (10)$$

where $K_{\mathrm{agg},0}$ is the value of K_{agg} at $[\mathrm{ADP}]=0$, and K_{diss} is the microscopic dissociation constant for the ADP-GDH complex. The K_{diss} value was found to be 0.52 ± 0.07 mM. It is reasonable to suppose that this value of K_{diss} corresponds to the temperature of 39.1°C.

Conclusion

This article has described a new approach to testing the agents affecting the stability of proteins. The approach is based on the quantitative analysis of the initial increment in the light scattering intensity caused by aggregation of the denatured protein molecules in the experiments where aggregation is studied in the regime of the elevation of temperature with a constant rate. The proposed approach allows estimating the temperature at which the initial increase in the light scattering intensity is registered (T_0) and establishing parameter K_{agg}, which characterizes the rate of aggregation. Temperature T_0 is a moment of the origination of the start aggregates. Such aggregation systems may be used for testing the compounds affecting protein stability as a result of direct binding to the native protein molecule (for example, substrates and modifiers of the enzymes); the compounds stabilizing the protein structure owing to the effects of excluded volume (for example, osmolytes); and the compounds possessing chaperone-like activity (for example, small heat shock proteins). If we want to select agents affecting exclusively the stage of denaturation, we should demonstrate that these agents have no effect on the stage of aggregation. In turn, this would require

Table 2. Parameters of aggregation of GDH (0.12 mg/ml) in the presence of different ligands (0.1 M Na-phosphate buffer, pH 7.6).

Ligand	T_0 (°C)	K_{agg} [(counts/s)·(°C)$^{-2}$]
-	34.3±0.1	(8.7±0.1)·10^2
NADH (0.2 mM)	35.0±0.1	(11.6±0.2)·10^2
NAD (0.2 mM)	34.5±0.1	(8.4±0.1)·10^2
ADP (0.5 mM)	39.3±0.1	(4.7±0.1)·10^2
NADH (0.2 mM)+ ADP(0.5 mM)	36.4±0.1	(4.7±0.1)·10^2
L-Leucine (50 mM)	36.0±0.1	(2.8±0.1)·10^2
L-Glutamate (50 mM)	32.8±0.1	(4.9±0.1)·10^2

doi:10.1371/journal.pone.0022154.t002

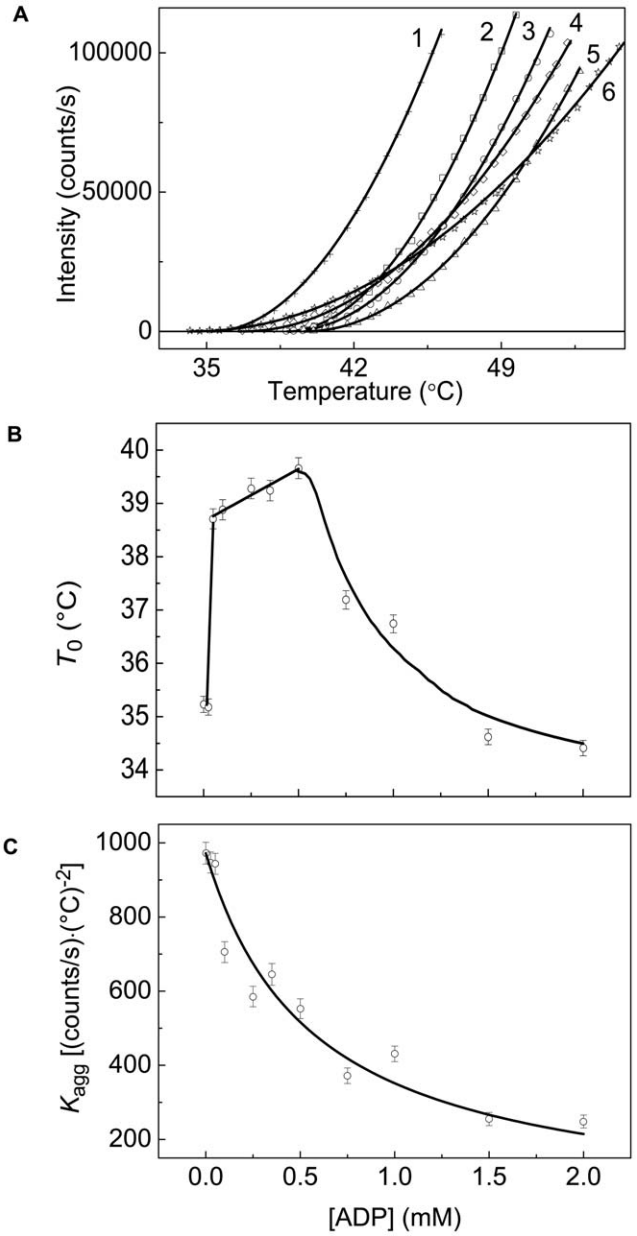

Figure 13. Effect of ADP on GDH aggregation. (**A**) The initial parts of the dependences of the light scattering intensity on temperature for aggregation of GDH (0.16 mg/ml) in the presence of the following concentrations of ADP: (1) 0, (2) 0.05, (3) 0.1, (4) 0.5 and (6) 2 mM. (**B** and **C**) The dependences of parameters T_0 and K_{agg} calculated from Eq. (4) on the ADP concentration, respectively. The solid curve in panel **C** was calculated from Eq. (10) at $K_{\mathrm{diss}}=0.52$ mM.
doi:10.1371/journal.pone.0022154.g013

additional aggregation systems where a preliminary denatured protein undergoes thermal aggregation. A protein denatured by ultraviolet radiation may be used for this purpose [64]. Test-systems based on aggregation of UV-irradiated proteins allow registering the direct action of the agents under study on the stages of aggregation.

When discussing the practical utility of the method of study of protein-ligand interactions proposed in the present work, we should like to note, first of all, that this method may be used for characterization of the proteins themselves. The results of investigation of protein stability in buffer solutions of different composition may be useful for selection of optimal buffer for purification procedure and storage of the proteins under study. The protein mutant forms obtained by genetic engineering may also be characterized by the method under discussion. Furthermore, screening against cofactors, substrate analogs, effectors and metals may be used to establish the conditions that favor protein stability. These stabilizing agents may be used during protein crystallization to improve the crystallization rate. Finally, an important line of application of the screening procedure based on the measurements of the light scattering intensity increase, which accompanies protein aggregation, is the search for compounds of potential medicinal significance.

Acknowledgments

The authors thank Igor Yudin for technical assistance.

Author Contributions

Conceived and designed the experiments: TE BK. Performed the experiments: TE OM VB SK RA. Analyzed the data: TE BK. Contributed reagents/materials/analysis tools: TE BK. Wrote the paper: TE BK. Engaged in active discussion: TE KM BK.

References

1. Senisterra GA, Markin E, Yamazaki K, Hui R, Vedadi M, et al. (2006) Screening for ligands using a generic and high-throughput light-scattering-based assay. J Biomol Screen 11: 940–948.
2. Senisterra GA, Ghanei H, Khutoreskaya G, Dobrovetsky E, Edwards AM, et al. (2010) Assessing the stability of membrane proteins to detect ligand binding using differential static light scattering. J Biomol Screen 15: 314–320.
3. Kurganov BI (1998) Kinetics of heat aggregation of proteins. Biochemistry (Mosc) 63: 364–366.
4. Eronina TB, Chebotareva NA, Bazhina SG, Makeeva VF, Kleymenov SY, et al. (2009) Effect of proline on thermal inactivation, denaturation and aggregation of glycogen phosphorylase *b* from rabbit skeletal muscle. Biophys Chem 141: 66–74.
5. Eronina TB, Chebotareva NA, Bazhina SG, Kleymenov SY, Naletova IN, et al. (2010) Effect of GroEL on thermal aggregation of glycogen phosphorylase *b* from rabbit skeletal muscle. Macromol Biosci 10: 768–774.
6. Maloletkina OI, Markossian KA, Asryants RA, Semenyuk PI, Kurganov BI (2010) Effect of 2-hydroxypropyl-β-cyclodextrin on thermal inactivation, denaturation and aggregation of glyceraldehyde-3-phosphate dehydrogenase from rabbit skeletal muscle. Inter J Biol Macromol 46: 487–492.
7. Maloletkina OI, Markossian KA, Belousova LV, Kleimenov SY, Orlov VN, et al. (2010) Thermal stability and aggregation of creatine kinase from rabbit skeletal muscle. Effect of 2-hydroxypropyl-β-cyclodextrin. Biophys Chem 148: 121–130.
8. Roberts CJ (2006) Non-native protein aggregation. Pathways, kinetics, and shelf-life prediction. In: Murphy RM, Tsai AM, eds. Misbehaving Proteins: Protein Misfolding, Aggregation, and Stability. New York: Springer. pp 17–46.
9. Weiss WFIV, Young TM, Roberts CJ (2009) Principles, approaches, and challenges for predicting protein aggregation rates and shelf life. J Pharm Sci 98: 1246–1277.
10. Kurganov BI, Kornilaev BA, Chebotareva NA, Malikov VP, Orlov VN, et al. (2000) Dissociative mechanism of thermal denaturation of rabbit skeletal muscle glycogen phosphorylase *b*. Biochemistry 39: 13144–13152.
11. Sabbaghian M, Ebrahim-Habibi A, Nemat-Gorgani M (2009) Thermal aggregation of a model allosteric protein in different conformational states. Int J Biol Macromol 44: 156–162.
12. Khanova HA, Markossian KA, Kurganov BI, Samoilov AM, Kleimenov SYu, et al. (2005) Mechanism of chaperone-like activity. Suppression of thermal aggregation of β_L-crystallin by alpha-crystallin. Biochemistry 44: 15480–15487.
13. De Young LR, Fink AL, Dill KA (1993) Aggregation of globular proteins. Acc Chem Res 26: 614–620.
14. Sugunakar YP, Przybycien TM (1996) Simulations of reversible protein aggregate and crystal structure. Biophys J 70: 2888–2902.
15. Speed MA, King J, Wang DIC (1997) Polymerization mechanism of polypeptide chain aggregation. Biotechnol Bioeng 54: 333–343.
16. Ferrone F (2003) Analysis of protein aggregation kinetics. Meth Enzymol 309: 256–274.
17. Wang K, Kurganov BI (2003) Kinetics of heat- and acidification-induced aggregation of firefly luciferase. Biophys Chem 106: 97–109.
18. Philo JS, Arakawa T (2009) Mechanisms of protein aggregation. Curr Pharm Biotechnol 10: 348–351.
19. Morris AM, Watzky MA, Finke RG (2009) Protein aggregation kinetics, mechanism, and curve-fitting: a review of the literature. Biochim Biophys Acta 1794: 375–397.
20. Chen S, Ferrone FA, Wetzel R (2002) Huntington's disease age-of-onset linked to polyglutamine aggregation nucleation. Proc Natl Acad Sci U S A 99: 11884–11889.
21. Ignatova Z, Gierasch LM (2005) Aggregation of a slow-folding mutant of a beta-clam protein proceeds through a monomeric nucleus. Biochemistry 44: 7266–74.
22. Cellmer T, Douma R, Huebner A, Prausnitz J, Blanch H (2007) Kinetic studies of protein L aggregation and disaggregation. Biophys Chem 125: 350–359.
23. Golub N, Meremyanin A, Markossian K, Eronina T, Chebotareva N, et al. (2007) Evidence for the formation of start aggregates as an initial stage of protein aggregation. FEBS Lett 581: 4223–4227.
24. Khanova HA, Markossian KA, Kleimenov SYu, Levitsky DI, Chebotareva NA, et al. (2007) Effect of α-crystallin on thermal denaturation and aggregation of rabbit muscle glyceraldehyde-3-phosphate dehydrogenase. Biophys Chem 125: 521–531.
25. Meremyanin AV, Eronina TB, Chebotareva NA, Kleimenov SY, Yudin IK, et al. (2007) Effect of α-crystallin on thermal aggregation of glycogen phosphorylase *b* from rabbit skeletal muscle. Biochemistry (Mosc) 72: 518–528.
26. Markossian KA, Golub NV, Khanova HA, Levitsky DI, Poliansky NB, et al. (2008) Mechanism of thermal aggregation of yeast alcohol dehydrogenase I. Role of intramolecular chaperone. Biochim Biophys Acta 1784: 1286–1293.
27. Noda L, Kuby SA, Lardy H (1955) ATP-creatine transphosphorylase. Meth Enzymol 2: 11505–11610.
28. Putilina T, Skouri-Panet F, Prat K, Lubsen NH, Tardieu A (2003) Subunit exchange demonstrates a differential chaperone activity of calf α-crystallin towards β_{LOW}- and individual γ-crystallins. J Biol Chem 278: 13747–13756.
29. Meremyanin AV, Eronina TB, Chebotareva NA, Kurganov BI (2008) Kinetics of thermal aggregation of glycogen phosphorylase *b* from rabbit skeletal muscle: mechanism of protective action of α-crystallin. Biopolymers 89: 124–134.
30. Kastenschmidt LL, Kastenschmidt J, Helmreich E (1968) Subunit interactions and their relationship to the allosteric properties of rabbit muscle phosphorylase *b*. Biochemistry 7: 3590–3607.
31. Scopes RK, Stoter A (1982) Purification of all glycolytic enzymes from one muscle extract. Meth Enzymol 90: 479–490.
32. Kirschenbaum DM (1972) Molar absorptivity and $A^{1\%}_{1cm}$ values for proteins at elected wavelengths of the ultraviolet and visible region. Int J Protein Res 4: 63–73.
33. Privalov PL, Potekhin SA (1986) Scanning microcalorimetry in studying temperature-induced changes in proteins. Meth Enzymol 131: 4–51.
34. Scientist for Experimental Data Fitting (1995) Microsoft Windows Version 2.0. Salt Lake City: Micro-Math Inc.
35. Markossian KA, Khanova HA, Kleimenov SY, Levitsky DI, Chebotareva NA, et al. (2006) Mechanism of thermal aggregation of rabbit muscle glyceraldehyde-3-phosphate dehydrogenase. Biochemistry 45: 13375–13384.
36. Markossian KA, Kurganov BI, Levitsky DI, Khanova HA, Chebotareva NA, et al. (2006) Mechanisms of chaperone-like activity. In: Obalinsky TR, ed. Protein Folding: New Research. New York: Nova Science Publishers Inc. pp 89–171.
37. Markossian KA, Yudin IK, Kurganov BI (2009) Mechanism of suppression of protein aggregation by alpha-crystallin. Int J Mol Sci 10: 1314–1345.
38. Chrunyk BA, Evans J, Lillquist J, Young P, Wetzel R (1993) Inclusion body formation and protein stability in sequence variants of interleukin-1β. J Biol Chem 268: 18053–18061.
39. Chrunyk BA, Wetzel R (1993) Breakdown in the relationship between thermal and thermodynamic stability in an interleukin-1β point mutant modified in a surface loop. Protein Eng 6: 733–738.
40. Raibekas AA (2008) Estimation of protein aggregation propensity with a melting point apparatus. Anal Biochem 380: 331–332.
41. Duy C, Fitter J (2005) Thermostability of irreversible unfolding alpha-amylases analyzed by unfolding kinetics. J Biol Chem 280: 37360–37365.

42. Li Y, Roberts CJ (2009) Lumry-Eyring nucleated-polymerization model of protein aggregation kinetics. 2. Competing growth via condensation and chain polymerization. J Phys Chem B 113: 7020–7032.
43. Markossian KA, Golub NV, Chebotareva NA, Asryants RA, Naletova IN, et al. (2010) Comparative analysis of the effects of alpha-crystallin and GroEL on the kinetics of thermal aggregation of rabbit muscle glyceraldehyde-3-phosphate dehydrogenase. Protein J 29: 11–25.
44. Panyukov Y, Yudin I, Drachev V, Dobrov E, Kurganov B (2007) The study of amorphous aggregation of tobacco mosaic virus coat protein by dynamic light scattering. Biophys Chem 127: 9–18.
45. Eronina TB, Chebotareva NA, Kleymenov SY, Roman SG, Makeeva VF, et al. (2010) Effect of 2-hydroxypropyl-β-cyclodextrin on thermal stability and aggregation of glycogen phosphorylase *b* from rabbit skeletal muscle. Biopolymers 93: 986–993.
46. Golub NV, Markossian KA, Sholukh MV, Muranov KO, Kurganov BI (2009) Study of kinetics of thermal aggregation of mitochondrial aspartate aminotransferase by dynamic light scattering: protective effect of alpha-crystallin. Eur Biophys J 38: 547–556.
47. Aymard P, Gimel JC, Nicolai T, Durand D (1996) Experimental evidence for a two-step process in the aggregation of beta-lactoglobulin at pH 7. J Chim Phys 93: 987–997.
48. Le Bon C, Nicolai T, Durand D (1999) Kinetics of aggregation and gelation of globular proteins after heat-induced denaturation. Macromolecules 32: 6120–6127.
49. Durand D, Gimel JC, Nicolai T (2002) Aggregation, gelation and phase separation of heat denatured globular proteins. Physica A 304: 253–265.
50. Baussay K, Bon LC, Nicolai T, Durand D, Busnel JP (2004) Influence of the ionic strength on the heat-induced aggregation of the globular protein beta-lactoglobulin at pH 7. Int J Biol Macromol 34: 21–28.
51. Pouzot M, Nicolai T, Durand D, Benyahia L (2004) Structure factor and elasticity of a heat-set globular protein gel. Macromolecules 37: 614–620.
52. Tomita S, Yoshikawa H, Shiraki K (2011) Arginine controls heat-induced cluster-cluster aggregation of lysozyme at around the isoelectric point. Biopolymers;doi: 10.1002/bip.21637.
53. Bumagina ZM, Gurvits BY, Artemova NV, Muranov KO, Yudin IK, et al. (2010) Mechanism of suppression of dithiothreitol-induced aggregation of bovine alpha-lactalbumin by alpha-crystallin. Biophys Chem 146: 108–117.
54. Bumagina Z, Gurvits B, Artemova N, Muranov K, Kurganov B (2010) Paradoxical acceleration of dithiothreitol-induced aggregation of insulin in the presence of a chaperone. Int J Mol Sci 11: 4556–4579.
55. Manno M, Craparo EF, Podestà A, Bulone D, Carrotta R, et al. (2007) Kinetics of different processes in human insulin amyloid formation. J Mol Biol 366: 258–274.
56. Ghosh P, Kumar A, Datta B, Rangachari V (2010) Dynamics of protofibril elongation and association involved in Aβ42 peptide aggregation in Alzheimer's disease. BMC Bioinformatics 11(Suppl 6): 1–19.
57. Kornilaev BA, Kurganov BI, Eronina TB, Livanova NB (1996) Effect of specific ligands on thermal inactivation of muscle glycogen phosphorylase *b*. Biochemistry (Mosc) 61: 628–634.
58. Kornilaev BA, Kurganov BI, Eronina TB, Livanova NB (1996) Thermal inactivation of skeletal muscle phosphorylase *b*: protective effect of the specific ligands. Biochem Mol Biol Int 38: 921–927.
59. Kornilaev BA, Kurganov BI, Eronina TB, Chebotareva NA, Livanova NB, et al. (1997) Mechanism of heat denaturation of muscle glycogen phosphorylase *b*. Mol Biol (Mosc) 31: 82–89.
60. Kornilaev BA, Kurganov BI, Livanova NB, Eronina TB, Orlov VN, et al. (1997) Heat resistance of muscle glycogen phosphorylase *b* in the presence of specific ligands. Doklady Biochemistry 1352: 1–3.
61. Bolen DW (2001) Protein stabilization by naturally occurring osmolytes. In: Murphy KP, ed. Methods in Molecular Biology, vol. 168: Protein Structure, Stability, and Folding. Totowa, USA: Humana Press. pp 17–35.
62. Chebotareva NA, Kurganov BI, Livanova NB (2004) Biochemical effects of molecular crowding. Biochemistry (Mosc) 69: 1239–1251.
63. Street TO, Bolen DW, Rose GD (2006) A molecular mechanism for osmolyte-induced protein stability. Proc Natl Acad Sci U S A 103: 13997–14002.
64. Muranov KO, Maloletkina OI, Poliansky NB, Markossian, Kleymenov SY, et al. (2011) Mechanism of aggregation of UV-irradiated β_L-crystallin. Exp Eye Res 92: 76–86.